M&C 2017 - International Conference on Mathematics & Computational Methods Applied to Nuclear Science & Engineering, Jeju, Korea, April 16-20, 2017, on USB (2017)

Practical Semi-Heterogeneous Method in Nodal Core Analysis

S.A. Groenewald, R.H. Prinsloo, O.M. Zamonsky, D.I. Tomašević

Necsa, P.O. Box 582, Pretoria, Gauteng, South Africa, 0001, Suzanne.Groenewald@necsa.co.za

Abstract – *Environmental errors introduced during cross-section generation is addressed in this work. A semi-heterogeneous embedded scheme is used to adjust cross-sections and discontinuity factors on-the-fly for full-core calculations. This scheme is tested on PWR and MTR benchmarks and test problems which exhibit environmental errors; while improving the accuracy of the solution significantly, it largely retains the performance advantage of traditional nodal methods.*

I. INTRODUCTION

Full core nodal diffusion calculations generally suffer from environmental errors introduced during the cross-section generation process. In this work a semi-heterogeneous embedded scheme is proposed as potential remedy, wherein a simplified embedded solution is used to calculate on-the-fly environmental corrections to both cross-sections and discontinuity factors. This semi-heterogeneous representation differs from the original heterogeneous transport problem, with regards to the level of spatial heterogeneity, energy representation and order of the solution operator. This scheme is tested on PWR and MTR benchmarks and test problems which exhibit environmental errors; while improving the accuracy of the solution significantly, it largely retains the performance advantage of traditional nodal methods.

II. BACKGROUND

Few-group homogenised cross-sections and discontinuity factors (collectively known as nodal equivalence parameters) tend to suffer from environmental dependency. For example, nodal equivalence parameters for fuel are typically generated from a transport calculation for a fuel assembly in an infinite lattice environment, but are used in full-core calculations where the fuel assemblies can be surrounded by other (sometimes neutronically very different) assemblies, effectively changing the boundary conditions to the problem.

Both the nodal cross-sections and discontinuity factors are prone to environmental errors. The detailed flux in an assembly is used as a weighting function to collapse cross-sections with. This flux will be different if the assembly is in a different environment, thus leading to different cross-sections. This environmental error (due to the heterogeneity) is often encountered in PWR calculations where fuel assemblies can have a very heterogeneous internal structure. Methods such as cross-section rehomogenisation [1] are used to address this error to a large extent.

The diffusiveness of the environment in which an assembly is placed will have an impact on the accuracy of the discontinuity factors in particular. For example, in an infinite lattice calculation no diffusion error is made in the calculation of the homogenised flux. Once this assembly is placed in a core environment we can potentially make an error when calculating the homogenised flux, since we use the diffusion approximation. The discontinuity factors for this assembly cannot correct this error, which was not present in the cross-section generation. This environmental error is typically an issue in MTR and PWR MOX type of reactors, where the core loading configuration can be very heterogeneous and one can encounter steep flux gradients on node interfaces.

Increasing the accuracy of full core reactor calculations is an area of active research. There exists a large number of calculational schemes that aim to address this environmental error in nodal equivalence parameters [1,2]. One option is to generate cross-section data in an exact core environment [3], thereby removing the environmental error. While this is possible for most non-loadable reactor components, it is not practical for loadable components such as fuel assemblies, which will see a different core environment after every shuffle. An alternative method must be used to address the environmental error in nodal equivalence parameters for fuel and other loadable assemblies.

In recent times embedded lattice calculations have been proposed to address environmental errors [4,5,6]. Full-core embedded transport calculations, in which a global nodal diffusion core calculation is coupled to a set of independent fixed source heterogeneous transport problems for each core position (via incoming partial currents) have been shown to match the accuracy of a standalone full-core transport solution. The fine scale spatial, angular and energy dependent incoming flux distribution to each core position are the unknowns to be resolved in an iterative coupled solution scheme. After the completion of each embedded calculation, equivalence theory [7] is applied to produce updated nodal equivalence parameters for the driver nodal diffusion solution, which in turn will feed the next iteration of embedded calculations with improved incoming partial currents. In such a scheme the nodal diffusion solution actually acts as an acceleration scheme to the transport solver.

However, such a coupled scheme still exhibits calculational running times comparable to that of a typical full-core transport solution and as such cannot be considered as a practical option for industrial core analysis. We propose

a semi-heterogeneous embedded scheme, where the aim is not to reproduce the full inter-assembly transport flux, but rather to produce corrections to node-averaged cross-sections and assembly side-averaged discontinuity factors, therefore reducing the environmental error which is inherent to the pre-calculated nodal equivalence parameters, while retaining nodal-like calculational times. In this context, the word "semi" is used to convey a simultaneous simplification in energy representation, spatial heterogeneity and potentially solution operator, as compared to the original lattice calculation in which the cross-sections were generated.

In previous work [8] the feasibility of this semi-heterogeneous embedded scheme was demonstrated. In this work we have made improvements to the calculational scheme and underlying codes. In particular, we reformulate a set of equations for the correction to nodal equivalence parameters and we improve the quality of the embedded solver by including P1 anisotropic scattering in the embedded nodal transport code [9]. We test this scheme on PWR and MTR type problems.

III. THEORY

Our interest is to formulate an embedded assembly representation which would allow node-averaged reaction rates and side-averaged leakages to be largely preserved, while correctly capturing the effect of moving the assembly to core positions where the diffusion error manifests differently. This suggests that some embedded transport solution would be needed (as opposed to simply using embedded diffusion), but that the geometric, material and energy representation of the assembly could potentially be significantly simplified.

We consider the following correction scheme. We start by postulating that the reference nodal equivalence parameters (assembly in reference environment, which is never pre-calculated) could be written for discontinuity factor f and nodal cross-section Σ as:

$$f^{ref} = f^{inf} + \Delta f \tag{1}$$

and

$$\Sigma^{\mathrm{ref}} = \Sigma^{\mathrm{inf}} + \Delta\Sigma \,. \tag{2}$$

Our aim is therefore to calculate these correction (Δ) quantities. We construct the transport problem for the infinite lattice eigenvalue calculation as:

$$L^{\mathrm{het}}\Psi_{\infty}^{\mathrm{het}} = 0 \tag{3}$$

and the transport problem for the reference (or colourset) problem as:

$$L^{\mathrm{het}}\Psi_{\mathrm{ref}}^{\mathrm{het}} = 0 \text{ , with bc } B^{\mathrm{het}}\Psi_{\mathrm{ref}}^{\mathrm{het}} = 0 \,. \tag{4}$$

We recall that f^{inf} in Eq. (1) is typically obtained from an equivalent diffusion calculation where specified net current boundary conditions (bc) and nodal cross-sections are used (in turn obtained from the solution of Eq. (3)). This equivalent diffusion problem can be written as:

$$H^{\mathrm{hom}}\Phi^{\mathrm{hom}} = 0 \text{ , with bc } B^{\mathrm{hom}}\Phi^{\mathrm{hom}} = J^{\mathrm{het}} \,. \tag{5}$$

Thereafter the side-averaged discontinuity factor can be calculated from

$$f = \frac{\Psi_{\mathrm{side}}^{\mathrm{het}}}{\Phi_{\mathrm{side}}^{\mathrm{hom}}} \,. \tag{6}$$

We now make the following important observation: Instead of obtaining the reference (or corrected) discontinuity factor (f^{ref}) from Eq. (1), we could solve for Eq. (5) with corrected boundary conditions, cross-sections and k-eff, then calculate f^{ref} from Eq. (6). In other words we construct and solve the corrected equivalent diffusion problem:

$$H_{\mathrm{ref}}^{\mathrm{hom}}\Phi_{\mathrm{ref}}^{\mathrm{hom}} = 0 \text{ , with bc } B^{\mathrm{hom}}\Phi^{\mathrm{hom}} = J_{\infty}^{\mathrm{het}} + \Delta J^{\mathrm{het}} \tag{7}$$

after which

$$f^{\mathrm{ref}} = \frac{\Psi_{\mathrm{side},\infty}^{\mathrm{het}} + \Delta\Psi_{\mathrm{side}}^{\mathrm{het}}}{\Phi_{\mathrm{side,ref}}^{\mathrm{hom}}} \tag{8}$$

or in the case of partial current discontinuity factors [10]:

$$f^{\mathrm{ref}} = 2\frac{\left(\mathrm{J}_{\mathrm{side},\infty}^{-,\mathrm{het}} + \Delta\mathrm{J}_{\mathrm{side}}^{-,\mathrm{het}}\right) + \left(\mathrm{J}_{\mathrm{side},\infty}^{+,\mathrm{het}} + \Delta\mathrm{J}_{\mathrm{side}}^{+,\mathrm{het}}\right)}{\Phi_{\mathrm{side,ref}}^{\mathrm{hom}}} \,.$$

In Eq. (7) $H_{\mathrm{ref}}^{\mathrm{hom}}$ is actually equivalent to H^{hom}, with the exception that the nodal cross-sections and k-eff provided as parameters to the diffusion solution are also corrected.

This approach reduces the need for calculating Δf in Eq. (1) to instead estimate the corresponding differences in the following transport solution quantities:

$$\Delta J^{\mathrm{het}} = J_{\mathrm{ref}}^{\mathrm{het}} - J_{\infty}^{\mathrm{het}} \tag{9}$$

$$\Delta\Psi_{\mathrm{side}}^{\mathrm{het}} = \Psi_{\mathrm{side,ref}}^{\mathrm{het}} - \Psi_{\mathrm{side},\infty}^{\mathrm{het}} \,. \tag{10}$$

Note that in our implementation the net current correction is treated additively and to ensure a positive flux, the flux correction is treated multiplicatively. Furthermore, we need an estimate for the reference environment k-eff as

well as the node-averaged flux. Our task then remains to estimate these quantities in a practical manner.

1. Estimating correction parameters

In attempting to estimate these correction parameters, we have two concerns:

- the solution of the transport problem for the environmental error requires the reference incoming partial currents; and
- this solution still represents a full embedded heterogeneous transport solution, which is too costly to perform in an embedded scheme.

To alleviate these concerns in a practical manner, we again consider that our goal is simply to obtain the correction terms for node and side-averaged quantities (actually nodal cross-sections, node-averaged flux, side-averaged current and side-averaged flux). To this end it is reasonable to expect that the operator L^{het} could be simplified in two ways and still capture the relevant average transport behaviour; firstly it is possible that the order of the operator could be somewhat simplified, and secondly (and most importantly) that the material and energy representation of the assembly itself could be simplified to a more homogeneous representation. We therefore consider that we aim to solve the simplified semi-heterogeneous transport problem for the original and reference environments, thus instead of Eqs. (3) and (4), we solve the eigenvalue problem in the original environment:

$$L_{\infty}^{\text{shet}}\,\Psi_{\infty}^{\text{shet}} = 0 \qquad (11)$$

and the fixed source problem for the reference (or colourset) problem as:

$$L_{\text{ref}}^{\text{shet}}\,\Psi_{\text{ref}}^{\text{shet}} = 0 \text{ , with bc } B^{\text{shet}}\Psi_{\text{ref}}^{\text{shet}} = 0 \text{ .} \qquad (12)$$

The two operators L_{∞}^{shet} and $L_{\text{ref}}^{\text{shet}}$ differ only in eigenvalue; in Eq. (11) an infinite lattice eigenvalue is calculated and in Eq. (12) the fixed source calculation uses the core eigenvalue.

This semi-heterogeneous problem does not by its nature yet define the level of simplification in L^{shet} (the nature and discretization of the operator) or operator $B^{\text{shet}}\,\Psi^{shet}$ (the spatial, energy and angular detail in the boundary conditions) which would be acceptable. The key factor is to capture the change in the relevant parameters between the original and actual core environment, for correcting the parameters required in Eq. (7).

2. Proposed scheme

In summary we then proceed by iterating over the following global-local embedded scheme until convergence of the nodal core diffusion power distribution:

1. Solve the semi-heterogeneous problem for each embedded node in the original lattice environment. This is needed only once and occurs before the first embedded iteration.
2. Solve the global nodal diffusion problem with cross-sections and discontinuity factors as available (first iteration from pre-calculated environment – typically infinite lattice). For this step we use a group-by-group SANM solver [11].
3. Solve a set of independent embedded semi-heterogeneous transport problems for each node in every global iteration, with the boundary conditions defined as core nodal incoming partial currents modulated by the distributional (angular, spatial, spectral) information from the neighbouring node's outgoing partial current (from the previous embedded transport sweep). For the embedded problem we use a nodal Sn solver with P1 anisotropic scattering, using cross-sections from an infinite lattice calculation [9].
4. Perform, for each embedded node, an equivalent diffusion solution, from which nodal discontinuity factors are calculated. Ideally, partial current discontinuity factors should be utilized, to ensure that the nodal solution recovers the transport partial currents, which in turn acts as incoming sources to the next iteration transport problems.
5. After steps 2 and 3 converge, use the obtained correction parameters to construct the corrected equivalent diffusion solution (Eq. (7)) for each node, and calculate updated node-average cross-sections and side-averaged discontinuity factors. Non-fuel components are assumed to have reference equivalence parameters, as their nodal equivalent parameters were generated in either a full-core or sufficiently accurate colourset.
6. Finally, we compare the obtained results with a reference full-core Serpent [12] calculation, which was also the code used to generate the infinite medium and reference non-fuel equivalence parameters.

The design of this scheme naturally includes the possibility to select which nodes should have an embedded representation. Thus, only nodes exhibiting an environmental error, as well as their direct neighbours, need to have embedded calculations performed. The embedded neighbour nodes are required purely to generate an incoming angular, spatial and spectral distribution for the node of interest.

It is preferable to apply partial current discontinuity factors (as opposed to flux discontinuity factors), since the incoming partial currents represent the fixed sources for the

next iteration's set of transport problems. On the other hand, the form of equivalence theory applied is limited to the choice of non-fuel (reflector), pre-calculated equivalence parameters, which are kept constant during the embedded scheme. This is needed to ensure that equivalence parameters on two sides of the same surface are defined consistently.

IV. MODEL DESCRIPTION

Both the heterogeneity of an assembly and the diffusiveness of its environment will contribute to the environmental error present in the nodal equivalence parameters for this assembly. We can divide our problem space into sections according to these "carriers" of the environmental error. In particular, we can use the categorization in Fig. 1 to assist in the definition of the semi-heterogeneous solution.

In Fig. 1, we categorise the sources of environmental error as either the level of non-diffusiveness of the actual core environment, or the level of heterogeneity of the assembly design. These properties would lead to a need for correcting, respectively, the discontinuity factor, the nodal cross-sections, or of course both when a heterogeneous assembly is moved to a non-diffusive core environment.

To illustrate this scheme, consider some two node (assembly) test problems from the various categories shown in Fig. 1. Firstly, in the category of non-diffusive and homogeneous, we consider two test problems.

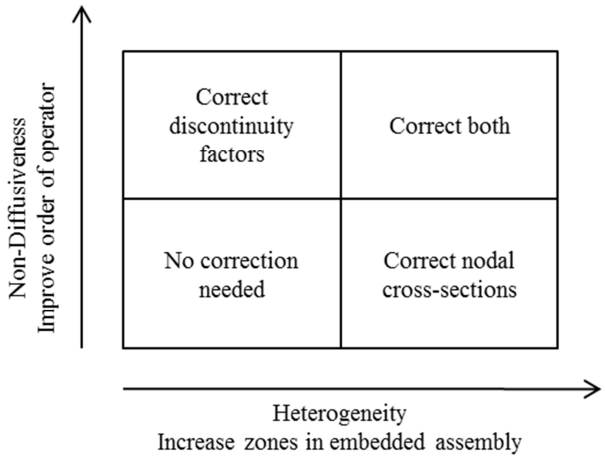

Fig. 1. Carriers of the environmental error

The first is a representative problem of the MTR-type reactor SAFARI-1. We construct a two node, six-group problem with a plate-type fuel assembly next to water, using reflective boundary conditions (as occurs on the pool-side of the reactor configuration). The fuel assembly is 7.71 cm wide and is rather homogeneous in design. The model is highly non-diffusive because of the neighbouring water reflector. The model is depicted in Fig. 2.

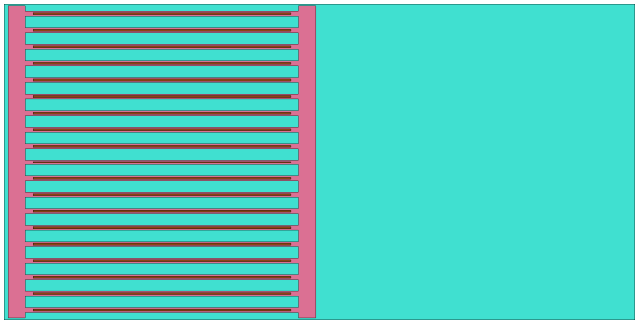

Fig. 2: MTR fuel / water model

Secondly, we investigate a two node example extracted from the C5G7 benchmark [13], modelling a UO2 assembly next to a water node in seven groups, with reflective boundary conditions. The two nodes are each 21.42 cm wide, and thus represent a much larger assembly. In both these cases we consider an embedded model represented by a single homogeneous set of cross-sections.

In the category of heterogeneous and non-diffusive, we consider a two node test problem consisting of a MOX assembly (from [13]) next to a water reflector, again in seven groups and using reflective boundary conditions. The MOX assembly is significantly more heterogeneous than the UO2 assembly, and here we will investigate the use of a three zone representation of the assembly in the embedded calculation (three equidistant zones, and thus three sets of cross-sections).

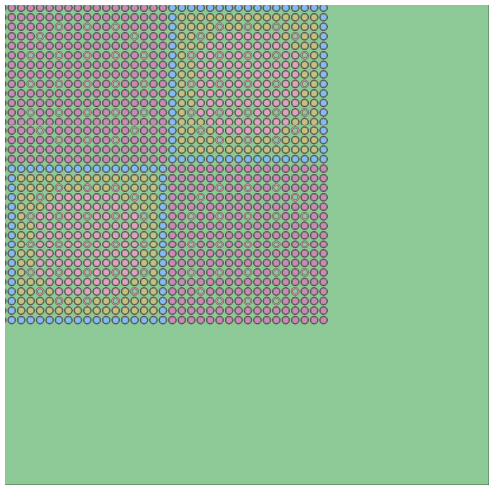

Fig. 3. The C5G7 benchmark model

Lastly, the primary numerical application problem in this paper is the 2D version of the well-known C5G7 benchmark problem. The detailed heterogeneous specification was largely taken from the recent NEA/OECD Time-dependent transport benchmark specification. This benchmark represents a particularly severe challenge with regards to environmental effects on both UO2 and MOX

fuel facing a water reflector on two sides. The C5G7 model is depicted in Fig. 3.

V. RESULTS

Results are given for various two node test problems, followed by the 2D version of the C5G7 power reactor benchmark.

1. Preliminary study of two node models

Prior to investigating the accuracy of the full scheme, it is instructive to analyse the capability of the scheme to predict the correction parameters (see Eqs. (9) and (10)). The actual results for these models are discussed in the next section.

The semi-heterogeneous scheme is applied to the two node MTR fuel / water model. We investigate the corrected net currents, surface and node-average flux, and k-eff (see Eqs. (9) and (10)), which in turn is used to recalculate the discontinuity factors for the fuel. The impact of our correction scheme on these quantities is illustrated in Fig. 4 to Fig. 6 and Tables I and II.

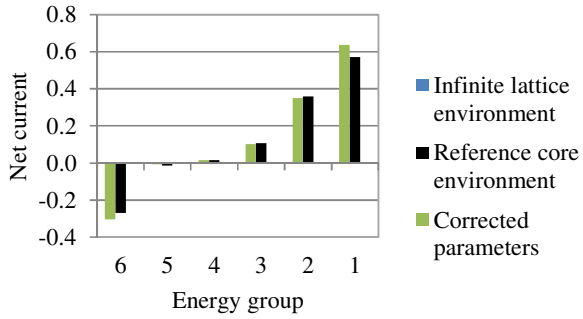

Fig. 4. Net current on fuel-water interface

The scheme improves the net current at the fuel-water interface from zero (in infinite lattice environment) to values with an error of less than 13 % relative to the net current in the reference core environment. This is illustrated in Fig. 4.

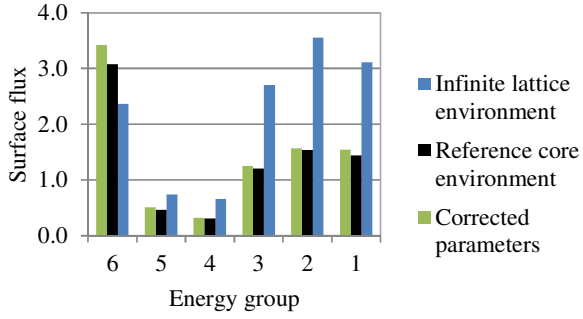

Fig. 5. Surface flux on fuel-water interface

From Fig. 5 and Fig. 6, a large difference is observed in surface and node averaged flux in the infinite lattice compared to the reference core environment. The spectrum is softer in the core environment, where the neighbouring water node thermalizes the neutrons.

The surface flux (Fig. 5) in fast groups for the infinite lattice environment shows more than 110 % error relative to the reference core environment. The scheme corrects the surface flux error to less than 5 %. This correction is somewhat smaller in the thermal groups, with original errors of 20 % and 60 % in groups 5 and 6 respectively, both group errors reducing to the order of 10 %. Similar behaviour is observed in the node average flux as illustrated in Fig. 6.

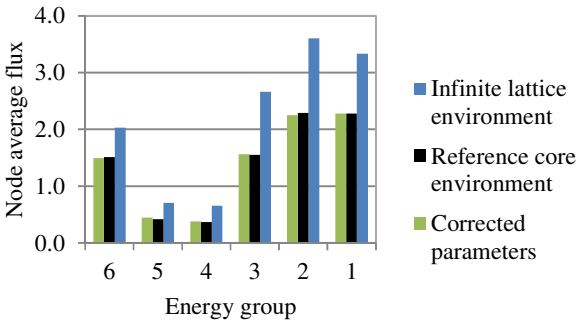

Fig. 6. Node average flux in fuel

The impact of the correction scheme on the discontinuity factors is illustrated in Table I. The discontinuity factors obtained through the correction scheme are more accurate than those from the infinite lattice environment only in energy groups 1, 2 and 4, with the largest improvement in group 1.

Table I: MTR fuel assembly discontinuity factor at fuel-water interface

Energy group	Reference disc. factor	Relative error (%)	
		Infinite lattice environment	Correction scheme applied
1	0.75	24.0	8.9
2	0.92	6.9	2.7
3	1.02	-0.6	1.6
4	1.05	-3.3	0.3
5	1.02	3.0	5.5
6	1.15	1.3	6.2

Considering a somewhat more complex case, we consider the UO2 / water interface from the 2D C5G7 problem. This case behaves in a similar manner and results for the discontinuity factors on the fuel-water interface for this assembly are given in Table II. The correction scheme significantly improves the discontinuity factor only in group 1.

From these results, we make an important observation. In all these problems, a comparison of the reference to infinite medium nodal parameters for the fuel assemblies in question shows that the primary contributor to the environmental error is the fast group discontinuity factor on the fuel-water interface. This is primarily due to the diffusion error on this boundary, and not to the actual error in homogenisation of the assembly.

Table II: C5G7 UO2 fuel assembly discontinuity factor at fuel-water interface

Energy group	Reference disc. Factor	Relative error (%)	
		Infinite lattice environment	Correction scheme applied
1	0.85	14.9	-3.7
2	1.00	-1.1	-8.9
3	1.02	-0.8	3.5
4	1.06	-3.1	4.4
5	1.06	-6.1	-2.2
6	1.01	-0.8	-8.5

Since the mean-free path of the neutrons in the fast group is roughly in the order of the assembly size, the fast flux solution through the assembly is quite well captured by a large homogeneous representation there-of, as was used in these cases. This observation naturally leads to the proposal of utilizing a relatively homogeneous representation of the assembly in the embedded model.

However, this further indicates that the nodal parameters in the lower energy groups would require a finer (more heterogeneous) semi-heterogeneous representation in space (in the order of their respective mean-free paths) to be well corrected.

Following this argumentation, results below include an option in which the semi-heterogeneous calculation is utilized only to correct the fast group parameters, as this is where the homogeneous assembly representation is expected to be most accurate, and more importantly, where the correction is most needed.

2. Two node models

Three small two node models are investigated, differing in fuel type, complexity and node size. In all cases, equivalence parameters for the water nodes are taken from the reference Serpent solution, while the fuel parameters are from an infinite lattice calculation, also from Serpent. Results for the embedded calculations are obtained with the scheme as discussed above. The reference calculation in Serpent is compared with:

1) Standard nodal solution with infinite lattice approximation for fuel element; and
2) Various embedded solutions, with accuracy tabulated for spatial refinement, angular order, and including the fast group correction option. The keyword GA implies that, after convergence of the scheme, all groups are corrected, while G1 implies that only group 1 is corrected.

P1 scattering order was used in all cases. Table III provides results for the two node MTR fuel / water model. In the base case (prior to any embedded calculations), an environmental error of 781 pcm exists. From this table we see a general improvement in almost all quantities as the scheme is applied. Due to the small size of the assembly, we do not investigate a multi-node representation of the MTR fuel model. As expected from the full homogeneous representation of the embedded node, the fast group correction is the most accurate, and sufficiently addresses the primary source of error.

Table III: 1D MTR fuel / water results

	k-eff error (pcm)	% Flux error in fuel (6 groups)	% Fast flux error in water
Serpent reference	1.16536	--	--
Nodal diffusion (infinite lattice)	781	4.4/5.5/2.8/ 0.7/1.6/5.1	14
Semi-het solution (1 node, S16, GA)	198	1.6/3.8/1.8/ 0.0/2.0/5.3	5.5
Semi-het solution (1 node, S16, G1)	67	1.9/4.8/2.2/ 0.2/1.8/5.1	5.3

We note that while the G1 option is somewhat less accurate in the fast group range than GA, it is more accurate in the thermal range and hence shows a k-eff improvement.

The UO2 case (see Table IV) illustrates a similar trend, but with a few notable differences. Given the larger size of the assembly, the overall environmental error of this problem is about half of that of the MTR case. Once again, due to the homogeneous nature of the UO2 assembly, no multi-zone representation of the assembly is considered.

Table IV: 1D UO2 / water results

	k-eff error (pcm)	% Flux error in fuel (7 groups)	% Fast flux error in water
Serpent reference	1.16254	--	--
Nodal diffusion (infinite lattice)	442	0.7/1.7/0.3/ 0.1/0.1/0.7/0.8	10
Semi-het solution (1 node,S16, GA)	320	0.1/1.1/0.1/ 0.3/0.2/0.7/0.6	2.2
Semi-het solution (1 node, S16, G1)	6	0.2/1.6/0.3/ 0.1/0.1/0.6/0.6	1.9

Our final two node problem is the MOX / water case, with results in Table V.

Firstly we note that the environmental error is elevated in comparison to the UO2 case. This is as expected since for

this case, both the homogeneous cross-sections and discontinuity factors are in need of correction. It is only once the assembly is subdivided into three homogeneous zones with different cross-sections that the accuracy notably improves. Here we notice that the GA option does reasonably well once the assembly is subdivided. However, given that the zone size is still large (7.14 cm), more zones would be needed to expect a notable improvement in the more thermal energies.

Table V: 1D MOX / water results

	k-eff error (pcm)	% Flux error in fuel (7 groups)	% Fast flux error in water
Serpent reference	1.05062	--	--
Nodal diffusion (infinite lattice)	561	0.5/1.6/0.1/ 0.4/0.6/1.1/0.1	9.1
Semi-het solution (1 node,S16, G1)	180	0.2/1.5/0.1/ 0.4/0.5/1.0/0.4	1.7
Semi-het solution (3 node,S16, GA)	142	0.0/1.1/0.5/ 0.5/0.6/0.9/0.4	1.7
Semi-het solution (3 node, S16, G1)	84	0.2/1.6/0.2/ 0.3/0.4/0.9/0.2	1.2

Once again the G1 correction proves most accurate, and since the discontinuity factors in the thermal groups are already well calculated in the original lattice calculation, they prove sufficient to capture local thermal effects on the side-averaged quantities.

3. C5G7 benchmark

This benchmark represents a particularly severe challenge with regards to environmental effects on both UO2 and MOX fuel facing a water reflector on two sides. Results are obtained with the scheme as discussed above, once again with reference eigenvalue and power distribution obtained from Serpent, and compared with:

1) Standard nodal solution with infinite lattice approximation for fuel elements; and
2) Various embedded solutions, with accuracy and timing comparisons tabulated as (spatial sub meshing, angular order, correction option, number of embedded iterations).

The semi-heterogeneous representation, used in each of the four fuel elements in the C5G7 embedded scheme, is a single node homogeneous cross-section set, P1 scattering and G1 option for the correction scheme. The spatial sub-meshing here refers to the number of computation meshes in the embedded calculation and not to further semi-heterogeneous cross-section zones.

Results are summarized in Table VI. From the table we notice a marked improvement in eigenvalue and maximum power error (which occurs in the corner UO2 assembly facing water on two sides). We observe that the S4 proves sufficient to capture the diffusion error on the water interfaces, and that four embedded iterations provides adequate feedback to the core calculation. The cases with ten and four embedded iterations converged to within 5 pcm and 15 pcm respectively.

The primary driver to the calculational time then remains the number of spatial mesh sub-meshes, for which the 4×4 subdivision provides the limiting improvement (6×6 shows no further error reduction).

Table VI: C5G7 results

	k-eff error (pcm)	Max assembly power error	Time
Serpent reference	1.17063	--	4 hours
Nodal diffusion (infinite lattice)	255	2.21 %	0.5s
Semi-het solution (4×4, S8, G1, 10)	74	0.85 %	200s
Semi-het solution (4×4, S4, G1, 10)	85	0.90 %	120s
Semi-het solution (4×4, S4, G1, 4)	57	0.91 %	25s
Semi-het solution (2×2, S4, G1, 4)	45	1.51 %	6s

The performance factors with 4×4 spatial sub-meshing is still somewhat outside the target performance criteria of about 10 times slower than a standard nodal calc.

However, at this stage of the test code implementation for the 2D calculation, spatially constant partial currents are shared on the boundaries of the embedded nodes per sub-mesh. Since the embedded code is a nodal Sn solver, it is in principle possible to share the spatial moments on the boundary, which would negate the requirement of spatial sub-meshing in the embedded calculation. This should achieve the target performance criteria.

VI. CONCLUSIONS

In this paper, further work regarding the development of a semi-heterogeneous embedded calculational scheme is described. The scheme aims to achieve a coarse mesh solution comparable in accuracy to the full embedded transport calculation, but at a fraction of the calculational cost. The semi-heterogeneous scheme is used as a correction model to the infinite lattice cross-sections and discontinuity factors. A series of 1D examples show the importance of correcting both the discontinuity factors and nodal cross-sections, depending on the nature of the problem. The C5G7 problem indicates that the approach performs well in 2D and on difficult PWR examples, and allows an initial estimate of calculational efficiency.

In this work the embedded representation was limited to large homogeneous zones, with the only exception being the 1D MOX example which utilized three sub-regions of different cross-sections. In future work, further studies will include finer sub-zoning to investigate the link between spatial and spectral corrections.

The results presented show good accuracy improvement, but the calculational efficiency is still slightly out of our requirements. However, the timing comparison for calculations without the need of spatial sub-meshing would in principle match the accuracy capability of our current calculations, but at a much shorter calculational time. This time will then be well within the defined target of no more than one order of magnitude slower than a standard nodal calculation. This is left for future work.

Additional future work would include the development of transport-to-transport equivalence for the multi-zone embedded solution. For the sake of improving calculational efficiency it is intended to enhance the embedded transport node-to-node coupling to include spatial moments instead of piece-wise constant angular fluxes.

REFERENCES

1. K.S. Smith, "Practical and Efficient Iterative Method for LWR Fuel Homogenization", *Trans. Am. Nucl. Soc*., **71**, 238 (1994).
2. M.R. Wagner, K. Koebke, J.H. Winter, "A Nonlinear Extension of the Nodal Expansion Method", *Proc. Conf. Advances in Math. Methods for the Solution of Nucl. Eng. Problems*, Munich, (1981).
3. B. Erasmus, et.al., "A Full Core Homogenization Approach Using Serpent as a Cross Section Generation Tool for the OSCAR-4 Code System", *Proc. RRFM 2015*, Bucharest, Romania, 19-23 April (2015).
4. P. Mondot, R. Sanchez, "An Iterative Homogenization Technique that Preserves Assembly Core Exchanges", *Proc. SNA 2003*, Paris, France, 22-24 Sept. (2003).
5. B. Ivanov, et.al., "Embedded Lattice Calculations Based on PARAGON-NEM Code System for Reactor Core Analysis", *Proc. PHYSOR 2008*, Interlaken, Switzerland, 14-19 September, 2008, American Nuclear Society (2008) (CD-ROM).
6. D.V. Colameco, *Next Generation Iterative Transport-Diffusion Methodology for LWR Core Analysis*, Ph.D. thesis, Penn. State University, Dept. of Nuclear Engineering (2012).
7. K.S. Smith, "Assembly Homogenization Techniques for Light Water Reactor Analysis", *Prog. in Nucl. Energy*, **17** (3), 303-335 (1986).
8. R.H. Prinsloo, et.al., "A Semi-Heterogeneous Method for On-the-Fly Environmental Correction of Nodal Equivalence Parameters", *Proc. MC 2015*, Nashville, TN, 19-23 April, 2015, American Nuclear Society (2015) (CD-ROM).
9. O.M. Zamonsky, Y.Y. Azmy, "Adaptive Order Nodal Transport Method", *Trans. Am. Nucl. Soc*., **78**, 132 (1998).
10. R. Sanchez, "Assembly Homogenization Techniques for Core Calculations", *Prog. in Nucl. Energy*, **51**, 14 (2009).
11. R.H. Prinsloo, D.I. Tomašević, H. Moraal, "A practical implementation of the higher-order transverse-integrated nodal diffusion method", *Annals of Nucl. Energy*, **68**, 70-88 (2014).
12. E. Fridman, J. Leppänen, "On the Use of the Serpent Monte Carlo Code for Few-Group Cross Section Generation", *Annals of Nucl. Energy*, **38**, 1399 (2011).
13. V.F. Boyarinov, et.al. "Deterministic Time-Dependent Neutron Transport Benchmark without Spatial Homogenization (C5G7-TD)", NEA/NSC/DOC(2016) (2016).